Real-Time 3D Electrical Impedance Imaging for Ventilation and Perfusion of the Lung in Lateral Decubitus Position

Tzu-Jen Kao, Bruce Amm, *Member, IEEE*, Xin Wang, Gregory Boverman, *Member, IEEE*, David Shoudy, James Sabatini, Jeffrey Ashe, Jonathan Newell, *Senior Member, IEEE*, Gary Saulnier, *Senior Member, IEEE*, David Isaacson *Senior Member, IEEE*, David Davenport

***Abstract*— We report a prototype Electrical Impedance Imaging System. It is able to detect the gravity-induced changes in the distributions of perfusion and ventilation in the lung between supine and lateral decubitus positions. Impedance data were collected on healthy volunteer subjects and 3D reconstructed images were produced in real-time, 20 frames per second on site, without using averaging or a contrast agent. Imaging data also can be reconstructed offline for further analysis.**

I. Introduction

Use of electrical impedance imaging or electrical impedance tomography (EIT) for thorax studies dates back to the late 1980's. Researchers have built sophisticated electrical impedance systems and reconstruction algorithms for studying lung function [1, 2]. A comprehensive technology review of lung applications can be found in [3, 4, and 5].

EIT is able to detect not only impedance changes in the thorax due to ventilation but also phasic changes in pulmonary blood volume with cardiac contraction. It is also a noninvasive, radiation-free technology and could be built as a low-cost and portable device. Therefore, EIT is well suited for use in long-term bedside lung function monitoring to assess pulmonary ventilation and perfusion, sometimes called V/Q matching [6].

The main challenge in this use is that the impedance signal can be corrupted by noise and artifacts, such as motion, which can lead to misinterpretation of data. Another challenge in imaging the pulmonary perfusion is that the impedance signal from perfusion is significantly smaller than the one from ventilation.

To address these challenges, different techniques have been used for EIT perfusion imaging, including averaging [7, 8, and 9], contrast agents [10, 11], frequency filtering [12, 13] and principal component analysis [14, 15]. Each of these techniques has its own strengths but also suffers from different drawbacks. We believe a better solution is to build a high-speed, high-precision system to improve the signal quality and reduce the need for post-processing.

The main focus of this paper is to demonstrate, using a prototype impedance system and a 3D analytical reconstruction algorithm [16, 17], the perfusion differences in a healthy human subject in various body postures. The images are directly reconstructed from measured voltages without any averaging, contrast agent or extra signal processing.

Research supported by Grant Number 1R01HL 109854-01 from the National Institutes of Health. The content is solely the responsibility of the authors and does not necessarily represent the official views of the National Institutes of Health.

Tzu-Jen Kao is with GE Global Research Center, Niskayuna NY 12309 USA. (phone:518-387-4003, e-mail: kao@ge.com)

Bruce Amm, David Shoudy, James Sabatini, Xin Wang, Gregory Boverman, Jeffrey Ashe, and David Davenport are with GE Global Research Center, Niskayuna NY 12309 USA.

Jonathan Newell, Gary Saulnier, David Isaacson are with the Department of Biomedical Engineering, Electrical Computer and Systems Engineering, Mathematical Sciences at Rensselaer Polytechnic Institute, Troy, NY 12180 USA (e-mail: newelj@rpi.edu, saulng@rpi.edu; isaacd@rpi.edu).

II. Methods

A. EIT System - GENESIS

Our prototype EIT system, called the General Electric Noninvasive Electrical Impedance Spectroscopy Imaging System (GENESIS) [18], is a multiple current source system working at 10 kHz. The instrument consists of 32 channels, each capable of independently driving currents and measuring voltages. For this study, canonical current patterns were employed as described in [2, 16, and 17].

The precision of the system is 16 bits with external loads (including cables, electrodes and a dummy load), and the maximum current amplitude is 0.11 mA_{RMS} with a working voltage range of 5 μV to +/- 2 volts, controllable by the operator. A similar hardware design was reported by Cook et al. in 1994 [19].

The user interface contains a one-step linear analytic reconstruction algorithm and has been used to reconstruct the distribution of the impedance changes in real-time at nearly 20 frames per second. A detailed description of the reconstruction algorithm can be found in [16, 17]. A brief summary of the reconstruction and verification with a 3D saline tank is reported in [20].

B. Study protocol

Thirty-two commercially available ECG electrodes were attached around the chest of a healthy human subject in 2 circular rings with approximately equal spacing. The electrodes were 3 cm in diameter. The distance between top and bottom rings was about 6 cm, center-to-center. The top ring of electrodes was placed at the fourth intercostal space and the bottom ring was placed at the sixth intercostal space. A safety ground electrode was placed on the subject's shoulder (back side, not visible in the figure 1) and connected to the system's safety circuit for detecting any unexpected leakage current. The system will switch off automatically if

the leakage current is greater than the threshold of 0.450 mA_{RMS}. Two ECG electrodes were placed on the upper region of subject's chest to measure the Lead I ECG signal.

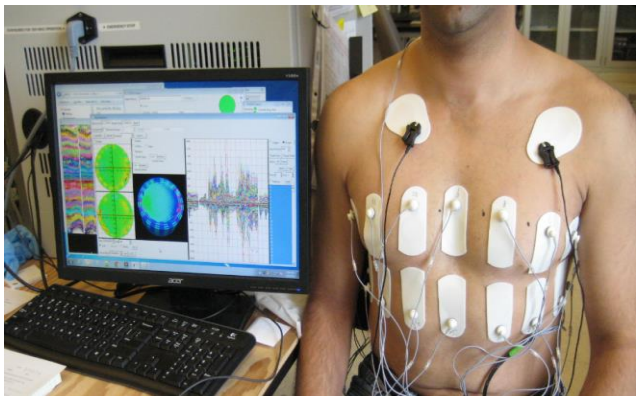

Figure 1: Prototype EIT system GENESIS and a healthy subject. (Note: The left side of the image is the display screen of the system with a user interface to display real-time reconstructed images. The main body of the system, 21 x 19.5 x 24.5 inches, is behind the screen.)

To better correlate to the breathing and cardiac cycles, the subject breathed through a pneumotachograph (Biopac, Goleta, CA) with a breathing mask and a pulse oximeter was placed on the right hand for photoplethysmograph (PPG) measurements. The pneumotachograph signal was integrated to obtain the "spirometer" signal, a measure of volume change at the airway. The subject was studied first upright, then supine, then left-lateral decubitus, then right lateral decubitus, and finally upright again. During the study, the subject performed a series of respiratory maneuvers in each posture: normal breathing (60 seconds), deep breathing (60 seconds), breath holding (30 seconds), and normal breathing again (30 seconds). To mimic mechanical ventilation with plateau curves in the spirometer waveform, the subject was asked to hold their breath for 1~2 seconds at the end of inspiration and expiration during the deep breathing cycle.

The 3D analytical reconstruction algorithm was embedded in the prototype GENESIS system. With the present hardware setup, the system generated and displayed reconstructed images at nearly 20 frames per second to monitor the subject in real-time.

III. Results

A. Global Conductivity Change

Figure 2 shows the correlation between the EIT global conductivity data and the spirometer and PPG data from one subject with a BMI of 23.5. The global conductivity value was calculated as the best constant approximation to the chest conductivity. A detailed derivation was given by Mueller et *al.* in 1999 [21].

To compare the timing of the PPG waveforms and the spirometer waveforms with the global conductivity changes in one figure, we normalized all waveforms to make the envelope of each waveform have the same amplitude. We also manually shifted the time axis to synchronize waveforms.

The curve of the global conductivity closely matches the spirometer curve during normal breathing, deep breathing and breath holding. To compare the PPG and global conductivity waveforms, we expanded the data during breath holding and plotted it at the bottom of Figure 2. The key finding is that global conductivity change matches the PPG waveform well, including during some premature heartbeats.

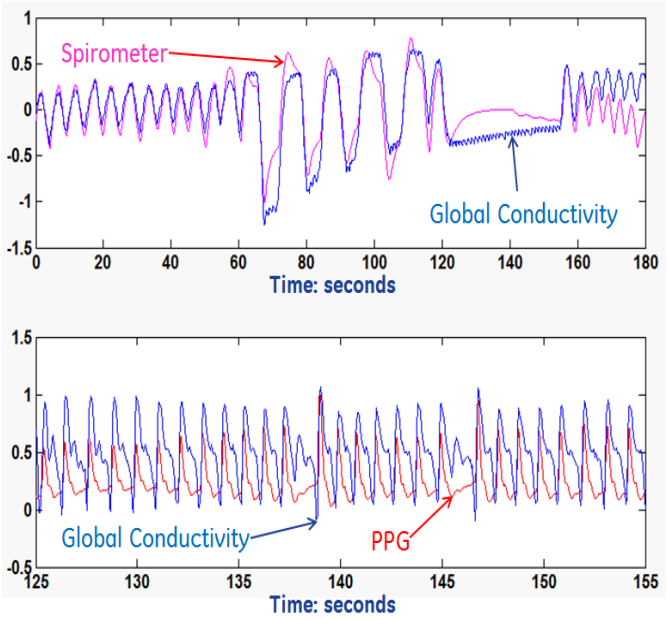

Figure 2: The top figure is Spirometer waveform vs. the global conductivity change. The bottom figure is PPG vs. the global conductivity at breath holding section (125th ~ 155th seconds)

B. Real-time Reconstructed Images

The real-time reconstructed perfusion and ventilation images from 3 different body postures (supine, left-lateral, right-lateral) are shown in Figure 3. Each reconstructed image is presented in 2 layers, top and bottom. The top layer represents the conductivity change of the cephalad electrode plane and the bottom represents the caudal electrode plane. The perfusion images all use the same color scale, and the ventilation images use another color scale. Red indicates an increase in conductivity from the chosen reference frame to the depicted frame and blue represents a decrease in conductivity. The perfusion images are reconstructed during breath-holding and are at end-systole with the reference frame being at end-diastole. The ventilation reference was at end-expiration, and the image is at end-inspiration. The images are in DICOM orientation – ventral is up, as viewed from the feet.

To verify the impedance signal of perfusion and ventilation, we analyzed the signals from selected voxels as shown in Figure 4. The Y axis is the conductivity difference in arbitrary units compared with the reference frame. The X axis is the number of the data frames, at nearly 20 frames/sec.

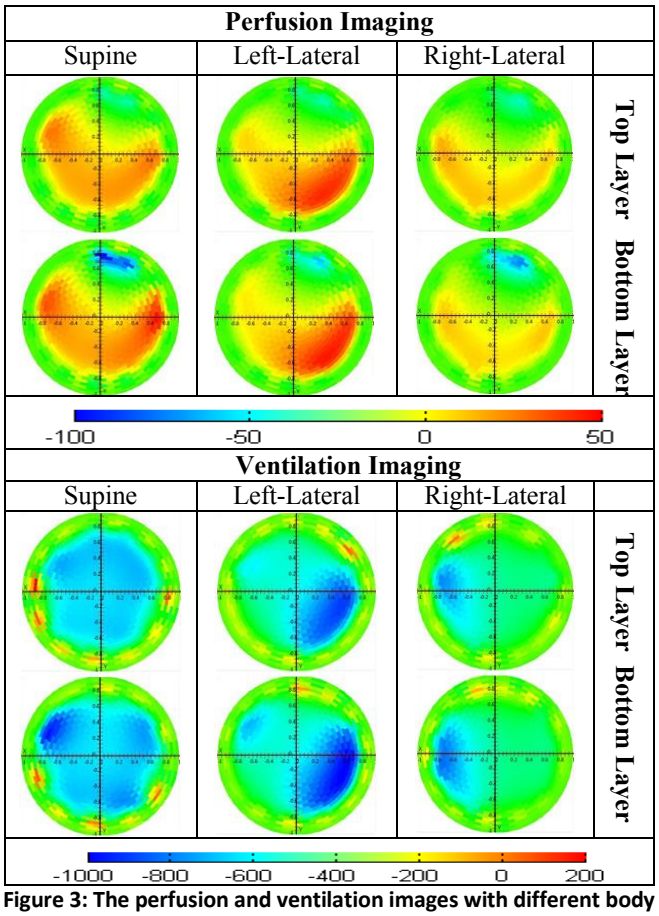

Figure 3: The perfusion and ventilation images with different body postures. The reconstructed images have different reference points for each case.

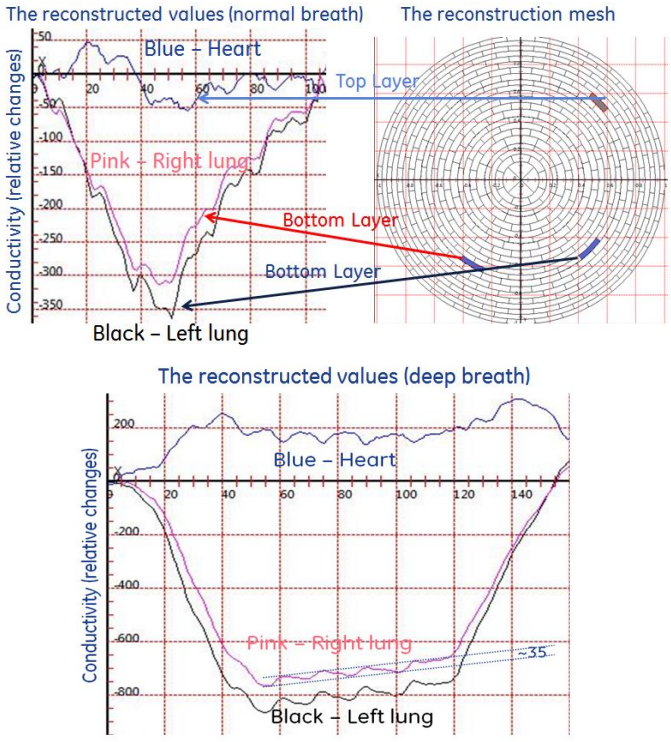

Figure 4: Top left: Reconstructed conductivity values for the voxels at the region of the right lung (Pink), left lung (black) and heart (blue) during one normal breath. Top right: The map of the reconstruction voxels. The bottom shows the reconstructed values during deep breathing.

IV. DISCUSSION

We analyzed the values from the reconstructed voxels at the regions of the lungs and heart shown in Figure 4. The signal change due to ventilation (700 ~ 850) in the lungs was about 20x that due to perfusion (30 ~ 40) in the lungs during deep breathing and about 10x during normal breathing (300 ~ 400). This ratio is consistent with the findings of Eyuboglu [22] and of Newell [23].

In Figure 3, the perfusion images show that in the left-lateral posture, the left lung area shows an increased conductivity signal and the right lung conductivity change decreases. The blood distribution is expected to be due to gravitational effects [24]; increasing blood flow to the dependent lung compared to the non-dependent lung. This phenomenon was found in the left-lateral posture and the right-lateral but the magnitude of the signal is stronger in the left-lateral than right lateral. It might be caused by the variation of the population in the anatomy and it will be studied more closely in future studies with more subjects.

This finding of greater ventilation in the dependent lung is as expected in spontaneous breathing [24]. This is due to the gravity gradient and to the fact that the lower diaphragm, on the dependent side, is able to contract more efficiently during spontaneous respiration (Figure 3).

Recently, Guerin et al. [25] studied 466 patients with severe Acute Respiratory Distress Syndrome (ARDS) who underwent prone-positioning sessions. They concluded that early application of prolonged prone-position sessions significantly improved the outcomes in patients' 28-day and 90-day mortality. It is possible that this result can be ascribed to regional changes in the distribution of pulmonary blood flow and/or ventilation. The apparatus described here may be able to verify this conjecture.

The 3D analytic reconstruction employed is designed on a cylindrical geometry which does not accurately represent the shape of a normal thorax. Therefore, there is some anatomical distortion in our real-time reconstructed images. A better geometry match to the subject's torso can be developed and processed off-line.

During this study, noise was observed in the reconstructed image close to the boundary. This might be caused by muscle contraction during breathing, as it was not as prevalent during breath holding, but will require further investigation. The quality of the reconstructed image is highly dependent on the choice of reference frame. For the ventilation images, a good choice of reference frame is the end of inspiration or expiration. For the perfusion image, during the breath hold, a good choice is at end-systole or end-diastole. In mechanical ventilation, the reference frames can be automatically chosen

by synchronizing the impedance system with the ventilator. Because of the high-speed and high-precision of GENESIS, a brief inspiratory hold is expected to be sufficient to catch 1 ~ 2 complete cardiac cycles for perfusion assessment.

V. Conclusion

We have demonstrated the ability of the GENESIS EIT prototype system to detect in real-time the gravity-induced changes in ventilation and perfusion without averaging or use of contrast media. The impedance measurements are highly correlated with Spirometer and photoplethysmograph (PPG) timing data. The ratio of the impedance signal from perfusion and ventilation is in good agreement with literature reports.

References

[1] Barber, D.C., Brown, B. H. 1984, Applied potential tomography. *J Phys Eng Sci Instrum* 17: 723-33.

[2] Newell, J.C., Gisser, D.G., Isaacson, D. 1988, An electric current tomograph. *IEEE Trans Biomed Eng.* 35(10):828-33.

[3] Brown, B. H. 2003, Electrical impedance tomography (EIT): a review. *J. Med. Eng. Technol.* 27: 97–108.

[4] Holder, D. S. 2005, Introduction to biomedical electrical impedance tomography Electrical Impedance Tomography Methods, History and Applications. Bristol: Institute of Physics pp. 423–49.

[5] Nguyen, D. T., Jin, C., Thiagalingam, A., McEwan, A. L. 2012, A review on electrical impedance tomography for pulmonary perfusion imaging *Physiol. Meas.* 33: 695.

[6] Leonhardt, S., Lachmann, B. 2012, Electrical impedance tomography: the holy grail of ventilation and perfusion monitoring? *Intensive Care Med* 38:1917–1929.

[7] Kunst, P.W., Vonk-Noordegraaf, A., Hoekstra, O.S., Postmus, P.E., De Vries, P.M. 1998, Ventilation and perfusion imaging by electrical impedance tomography: a comparison with radionuclide scanning. *Physiol. Meas.* 19: 481-90.

[8] Smit, H.J., Vonk-Noordegraaf, A., Marcus, J.T., Van Der Weijden, S., Postmus, P.E., De Vries, P.M., Boonstra, A. 2003, Pulmonary vascular responses to hypoxia and hyperoxia in healthy volunteers and COPD patients measured by electrical impedance tomography. *Chest* 123:1803-9.

[9] Smit, H.J., Handoko, M.L., Vonk-Noordegraaf, A., Faes, T.J., Postmus, P.E., De Vries, P.M., Boonstra, A., 2003, Electrical impedance tomography to measure pulmonary perfusion: is the reproducibility high enough for clinical practice? *Physiol. Meas.* 24: 491-9.

[10] Borges, J. B. *et al* 2011, Regional lung perfusion estimated by electrical impedance tomography in a piglet model of lung collapse. *J. Appl. Physiol.* 112:225–36.

[11] Frerichs, I., Hinz, J., Herrmann, P., Weisser, G., Hahn, G., Quintel, M., Hellige, G., 2002, Regional lung perfusion as determined by electrical impedance tomography in comparison with electron beam CT imaging. *IEEE Trans. Med. Imaging* 21:646–52.

[12] Frerichs, I., Pulletz, S., Elke, G., Reifferscheid, F., Schadler, D., Scholz, J., Weiler, N. 2009, Assessment of changes in distribution of lung perfusion by electrical impedance tomography. *Respir.* 77:282–91.

[13] Grant, C. A., Pham, T., Hough, J., Riedel, T., Stocker, C., Schibler, A. 2011, Measurement of ventilation and cardiac related impedance changes with electrical impedance tomography. *Crit. Care* 15:R37.

[14] Pikkemaat, R., Leonhardt, S. 2010, Separation of ventilation and perfusion related signals within EIT-data streams. *J. Phys. Conf.* Ser. 224:012028.

[15] Deibele, J. M., Luepschen, H., Leonhardt, S. 2008, Dynamic separation of pulmonary and cardiac changes in electrical impedance tomography. *Physiol. Meas.* 29:S1–14.

[16] Blue, R.S., 1997, Real-Time Three-Dimensional Electrical Impedance Tomography, Ph.D. Thesis, Rensselaer Polytechnic Institute, Troy, NY, USA.

[17] Blue, R.S., Isaacson D., Newell J.C., 2000, Real-time three-dimensional electrical impedance imaging. *Physiol. Meas.* 21:1-12.

[18] Ashe, J. M., Shoudy D., Boverman, G., Sabatini, J., Kao, T.-J., and Amm, B. 2014, A .High Precision Parallel Current Drive Experimental EIT System. 15th International Conference on Biomedical Application of EIT, pp. 24-26.

[19] Cook, R. D., Saulnier, G. J., Gisser, D. G., Goble, J. C., Newell, J. C., Isaacson, D., 1994, ACT3: A High-speed, High-Precision Electrical Impedance Tomograph. *IEEE Trans on Biomed Eng,* vol. 41, no. 8, pp. 713-722.

[20] Amm, B., Kao, T.-J., Wang, X., Boverman, G., Shoudy, D., Sabatini J., Ashe, J. M., Newell, J.C., Isaacson, D., Saulnier, G. J. Davenport, D. 2014, Real-Time 3D Electrical Impedance Imaging for Ventilation Monitoring of the lung: Pilot study. *IEEE EMBC* 36th Conf. Chicago (accepted).

[21] Mueller, J. L., Isaacson, D., Newell, J. C. 1999, A reconstruction Algorithm for Electrical Impedance Tomography Data Collected on Rectangular Electrode Array. *IEEE Trans. Biomed. Eng*., 46(11): 1379-1386.

[22] Eyuboglu, B. M., Brown, B. H., Barber, D. C. 1989, In vivo imaging of cardiac related impedance changes. *IEEE Eng. Med. Biol. Mag.* 8 39–45.

[23] Newell, J.C., Blue, R.S., Isaacson, D., Saulnier, G. J., Ross, A.S. Phasic 2001, Three-Dimensional Impedance Imaging of Cardiac Activity. *Proc 3rd EPSRC Conf. London*.

[24] Tobin, Martin, J. 2012, Principles and Practice of Mechanical Ventilation, Third Edition, McGraw-Hill, pp. 306.

[25] Guérin, C., Reignier J. et al, 2013, Prone Positioning in Severe Acute Respiratory Distress Syndrome. *N Eng J Med* 368:23.